

# Nonlinear effects in the propagation of optically generated magnetostatic volume mode spin waves

L.J.A. van Tilburg,<sup>1,\*</sup> F.J. Buijnsters,<sup>1</sup> A. Fasolino,<sup>1</sup> T. Rasing,<sup>1</sup> and M.I. Katsnelson<sup>1</sup>

<sup>1</sup>*Radboud University, Institute for Molecules and Materials,  
Heyendaalseweg 135, 6525AJ Nijmegen, The Netherlands*

(Dated: December 3, 2024)

## Abstract

Recent experimental work has demonstrated optical control of spin wave emission by tuning the shape of the optical pulse (Sato et al. *Nature Photonics*, 6, 662 (2012)). We numerically reproduce these results and expand the scope of the control by investigating nonlinear effects. We observe the generation of higher harmonics, leading to short-wavelength excitations and a pronounced asymmetry. In the nonlinear regime we observe self-focusing of the spin waves, generally described by the nonlinear Schrödinger equation. These observations open a way for the manipulation of magnetic structures at a smaller scale than the beam focus, for instance in devices with all-optical control of magnetism.

PACS numbers: 75.30.Ds, 78.20.Ls, 75.78.Cd

## I. INTRODUCTION

The study of propagating spin waves, collective excitations of the magnetization, is a subject of great interest in the emerging field of spintronics as they can be used in magnetic switching<sup>1</sup>, manipulation of domain walls<sup>2</sup> and logic devices<sup>3</sup>. One way of generating spin waves in a magnetic system is by means of the inverse Faraday effect (IFE).<sup>4-6</sup> In insulators with sizeable spin-orbit coupling, a circularly polarized light pulse induces a magnetic field pulse  $\mathbf{H}_{\text{ind}} \propto \mathbf{E} \times \mathbf{E}^*$  where  $\mathbf{E}$  is the electrical component of the incident light. The induced field is directed along the wavevector  $\mathbf{k}$  of the light. The IFE is based on an impulsive Raman scattering process and does not rely on absorption.<sup>7</sup> Thus, the effect can be used to excite spin waves at high fluence without depositing any heat in the system.

Recent experiments by Satoh *et al.*<sup>8</sup> on the ferrimagnetic garnet  $\text{Gd}_{4/3}\text{Yb}_{2/3}\text{BiFe}_5\text{O}_{12}$  have demonstrated directional control of the spin wave emission pattern. Garnets are particularly suitable for optical spin-wave experiments because many of them have a large magneto-optical response and relatively low spin wave damping.<sup>9</sup> Since the magnetization couples so strongly to the optical field, garnets are ideal to study nonlinear effects of the spin wave propagation, such as self-focusing: the concentration of the spin wave power at a single point.

Nonlinear effects of magnetostatic spin waves have a relatively low exciting threshold due to the low value of the ratio of dispersion and diffraction.<sup>10,11</sup> Previous studies of self-focusing spin waves relied on a microwave antenna to generate the spin waves. Nonlinear spin wave flow along a (quasi) one dimensional sample showed self-channeling of the spin waves.<sup>12-14</sup> For spin waves propagation in two dimensions, Brillouin light-scattering experiments showed spin wave focusing into quasi-stable ‘bullets’.<sup>10,11,15</sup> However, optically generated spin waves have not yet been studied in the nonlinear regime. All-optical experiments in a pump-probe setup can provide higher spacial and temporal resolution, enabling a far more detailed analysis of the spin wave dynamics. Here, we study the propagation of large amplitude spin waves by solving the Landau-Lifshitz-Gilbert equation. This approach allows to extend the current understanding to the nonlinear regime.

This article is organized as follows. In Sec. II we introduce the system under study and explain our numerical approach. In Sec. III we present numerical results of the spin wave propagation. Sec. III A deals with the linear regime (small initial excitations) where one can derive the spin wave dispersion (III A 1). We also present typical spin wave patterns that an optical pulse excites (III A 2) and compare them to experimental data. Sec. III B expands the scope to large initial excitations and presents results for nonlinear spin wave dynamics. In Sec. IV we summarize our results and discuss experimental feasibility of these nonlinear effects.

## II. METHOD

We are interested in the spin wave pattern that emerges when we prepare our system in an initial configuration at  $t = 0$  and calculate the time evolution by integrating the Landau-Lifshitz-Gilbert equation (LLG)<sup>16</sup>

$$\frac{\partial \mathbf{m}}{\partial t} = -\gamma (\mathbf{m} \times \mathbf{H}_{\text{eff}}) + \frac{\alpha}{m} \left( \mathbf{m} \times \frac{\partial \mathbf{m}}{\partial t} \right), \quad (1)$$

where  $\mathbf{m}$  is defined as the magnetization vector per volume,  $\gamma$  is the gyromagnetic ratio,  $\alpha$  is the Gilbert damping parameter and  $\mathbf{H}_{\text{eff}}$  is the effective magnetic field, calculated as the functional derivative of the energy with respect to the magnetization. The first term on the r.h.s. of Eq. 1 describes a precessional motion of the magnetization around the effective magnetic field. The second term describes the damping of this precession, ultimately aligning the magnetization to the field. We consider the following Hamiltonian

$$\mathcal{H}_{\text{tot}} = \mathcal{H}_{\text{ani}} + \mathcal{H}_{\text{dip}} + \mathcal{H}_{\text{Z}}, \quad (2)$$

for a uniform slab of thickness  $L$  of a material with out-of-plane easy-axis magnetic anisotropy  $\mathcal{H}_{\text{ani}} \sim K(\mathbf{m} \cdot \hat{\mathbf{e}}_z)^2$  where  $\hat{\mathbf{e}}_z$  is the normal to the surface. Magnetostatic dipole-dipole interactions are taken into account in the  $\mathcal{H}_{\text{dip}}$  term and  $\mathcal{H}_{\text{Z}} \sim M_S H_Z^x$  represents the Zeeman energy for an in-plane static external magnetic field which defines the equilibrium magnetization  $M_S$  along  $\hat{\mathbf{e}}_x$ . Since the exchange length,  $l_{\text{ex}} \propto \sqrt{A/M_S^2}$  with  $A$  the exchange constant, for garnets is of the order of nanometers, it is very small compared to the typical wavelengths of magnetostatic waves.<sup>17</sup> Therefore, we neglect the contribution of exchange. This defines the applicability of our approach as long as the wavelength  $2\pi/k$  of the spin waves is large compared to  $l_{\text{ex}}$  i.e.  $kl_{\text{ex}} \ll 1$ .

We solve Eq. 1 on a  $2400 \times 2000$  square lattice of macrospins with lattice parameter  $a = 1\mu\text{m}$  and periodic boundary conditions.<sup>18</sup> We fix the spin wave profile in the direction normal to the plane to be uniformly distributed (the uniform mode approximation). This approximation enables us to simulate the system as effectively two dimensional, greatly decreasing computational costs. Since the lowest order profile of the volume modes is homogeneous throughout the sample, this approximation is also effective beyond the thin-film limit.<sup>19</sup> The thickness  $L$  of the sample defines the intrinsic lengthscale in the simulation. To be able to capture the magnetization dynamics, we have taken care that the resolution is much smaller than this length scale ( $a \ll L$ ).

Since the period of the typical spin waves dynamics in our system is much longer than the pulse duration of the incident light, the effect of the optical field can be considered as instantaneous. Thus, in accordance with Eq. 1, for light at normal incidence the IFE leads to a tilt of the magnetization over an angle  $\theta$  in the direction of  $-(\mathbf{m} \times -\hat{\mathbf{e}}_z)$  i.e. a clockwise rotation around  $\hat{\mathbf{e}}_z$ . The profile of the optical pulse determines the spatial extent of the tilted spins. In this paper we consider the tilt angle profiles having the shape

$$\theta(x, y) = -\vartheta \exp\left(-\frac{x^2}{2x_0^2} - \frac{y^2}{2y_0^2}\right), \quad (3)$$

where  $x_0$  and  $y_0$  determine the ellipticity of the laser spot and the minus sign gives the rotation direction. Pulses with  $x_0 \neq y_0$  can be achieved by using an aperture as is done in Ref. 8. The angle  $\vartheta$  modulates the amplitude of the tilt of the excited state. A strong induced field due to the IFE effect would result in a large value for  $\vartheta$ . Since  $|\mathbf{m}|/M_S = 1$ , the local magnetization after the pulse is given by

$$\mathbf{m}_\vartheta(x, y) = \cos \theta \hat{\mathbf{e}}_x + \sin \theta \hat{\mathbf{e}}_y. \quad (4)$$

Figure 1 shows the systems geometry and two excited states as result of the laser pulse for different values of  $\vartheta$ .

The calculations were performed with a micromagnetics code developed in Nijmegen. The numerical integration follows the implicit-midpoint scheme (IMP) which conserves the magnitude of the initial spins.<sup>20</sup> A second property of this integration scheme is that it exactly conserves energy for Hamiltonians that are of quadratic order in the magnetization when damping is zero  $\alpha = 0$ .<sup>21</sup>

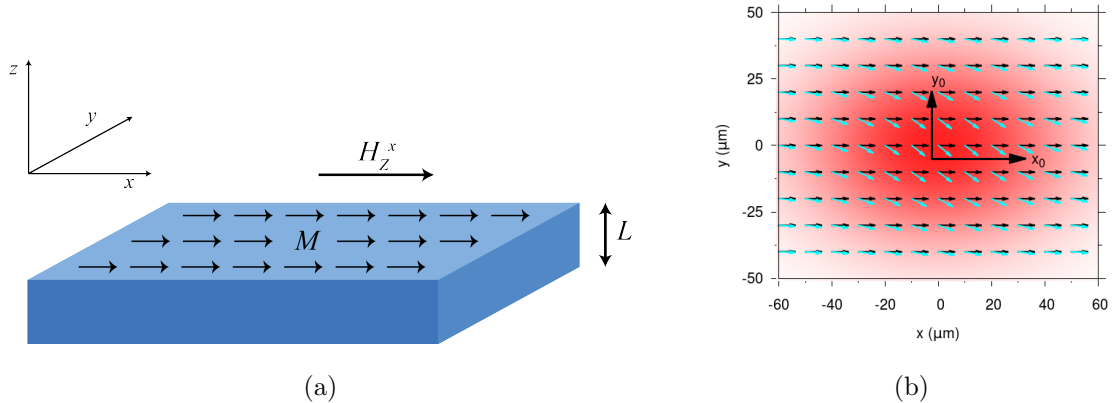


FIG. 1. A slab of material of thickness  $L$  with an external field  $H_Z^x$  along the  $x$  axis to align the in-plane magnetization: (a) system geometry and state before illumination; (b) top view of the excited state of the in plane magnetization after a pulse with  $x_0 = 35 \mu\text{m}$  and  $y_0 = 25 \mu\text{m}$  and varying laser intensities, according to Eq. 4. The red background shows the intensity profile of the optical field. The small vectors show the magnetization for  $\vartheta = 1^\circ$  (black) and  $\vartheta = 40^\circ$  (light blue).

### III. RESULTS

#### A. The linear regime ( $\vartheta = 1^\circ$ )

##### 1. The uniform mode dispersion

If we assume a uniform spin wave profile throughout the depth of the material, the dipole-dipole term in the Hamiltonian of Eq. 2 simplifies and can be treated analytically.<sup>19,22,23</sup> When the amplitude of the initial excitation  $\vartheta$  is small, it is possible to linearize the Landau-Lifshitz equation without damping and calculate the dispersion  $\omega$  of a spin wave with wavevector  $\mathbf{k}$

$$\omega(\mathbf{k}) = \mu_0 |\gamma| \sqrt{\left( H_Z^x + M_S \frac{k_y^2 e^{-kL} + kL - 1}{kL} \right) \left( \left( H_Z^x + M_S \frac{1 - e^{-kL}}{kL} \right) - \frac{2K}{\mu_0 M_S} \right)}, \quad (5)$$

with  $k^2 = k_x^2 + k_y^2$ . For spin waves parallel to the equilibrium magnetization ( $\mathbf{k} \parallel \mathbf{M}$ ) the dispersion reduces to the well known result for volume spin waves in thin films.<sup>11,24</sup>

Figure 2 shows the dispersion relation of Eq. 5 along the x- and y-axis, using the parameters from table I.

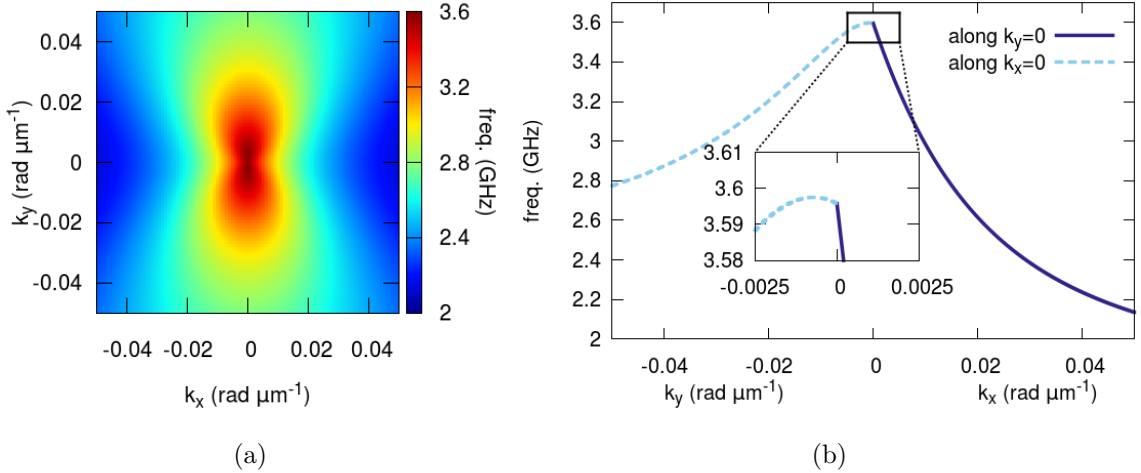


FIG. 2. The dispersion relation for magnetostatic volume mode spin waves in the  $xy$ -plane according to Eq. 5: (a) shows the dispersion in the full 2D plane; (b) shows a cut through momentum space along  $k_x$  (solid dark blue line) and  $k_y$  (dashed light blue line). The waves propagating along the external field  $H_z^x$  all have a negative group velocity. Waves propagating perpendicular to the field have a different behavior for small  $k$ .

For almost all wavevectors  $|\mathbf{k}|$ , the dispersion has negative slope. The associated spin waves are called backward volume magnetostatic waves (BVMSW) due to their negative group velocity. Only for very small values of  $k_y$ , the slope of the dispersion starts out positive, changing sign when  $k_y$  increases. This maximum in the dispersion results from our uniform mode approximation and disappears when the spin wave profile is allowed to vary in the  $z$ -direction.<sup>19</sup> In that case, the dispersion starts out flat for small  $k_y$ , decreasing when  $k_y$  increases.

## 2. Spin wave patterns

The propagation of optically generated spin waves in the linear regime has recently been studied using a pump-probe technique by Satoh *et al.*<sup>8</sup>. To assert the validity of our numerical scheme, that relies on the uniform mode approximation, we have calculated the spin wave patterns for the experimental parameters from Ref. 8. Figure 3 shows three snapshots of the spin wave pattern at  $t = 1.5$  ns for the excited state given by Eq. 4 at  $\vartheta = 1^\circ$ . The size and shape of the pump spot is varied using the parameters  $x_0$  and  $y_0$ . There is very good agreement with Figures 2a,b and 3b,c,e,f from Ref. 8, affirming that our numerical scheme

works well in calculation the spin wave propagation. We would like to emphasize that the calculations of spin wave patterns presented in Ref. 8 use a different method than the one employed by us. In Ref. 8 the instantaneous magnetization is calculated by integrating the Fourier transform of the initial excitation in time. In this integral the lowest order mode of the spin wave dispersion was used as input. It has been shown<sup>19</sup> that the lowest order dispersion gives a uniform depth profile of the spin waves for small  $\mathbf{k}$  and thus it is not surprising that our calculation and the calculation presented in Ref. 8 agree.

$M_S = 91 \text{ kA/m}$	$\gamma = 1.76 \cdot 10^{11} \text{ rad T}^{-1}\text{s}^{-1}$
$H_Z^x = 99 \text{ kA/m}$	$\alpha = 0.02$
$H_{\text{ani}} = 77 \text{ kA/m}$	$L = 110 \text{ }\mu\text{m}$

TABLE I. Numerical parameters used in the simulations. The value of the anisotropy field is a factor two higher than the experimental value listed in Ref. 8. The need for rescaling of the anisotropy can be attributed to the uniform mode approximation.<sup>19</sup>

See Supplemental Material at [URL will be inserted by publisher] for a video showing the spin wave dynamics after illumination of the sample with a circular spot  $x_0 = y_0 = 25 \text{ }\mu\text{m}$  and  $\vartheta = 1^\circ$ .

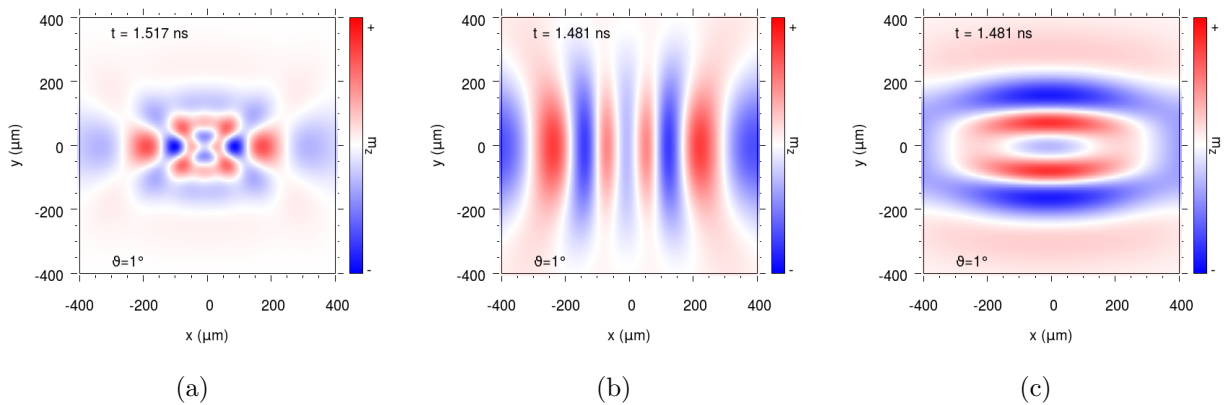


FIG. 3. Three snapshots of the spin wave pattern calculated at  $t = 1.5 \text{ ns}$ : (a) with a circular initial excitation  $x_0 = y_0 = 25 \mu\text{m}$  (top left); (b) with an elliptical initial excitation  $x_0 = 35 \mu\text{m}$ ,  $y_0 = 140 \mu\text{m}$ ; (c) with  $x_0 = 140 \mu\text{m}$ ,  $y_0 = 35 \mu\text{m}$ . These values have been chosen so that the spin wave patterns can be compared to data in Ref. 8

## B. The nonlinear regime ( $\vartheta > 1^\circ$ )

In contrast to the calculation presented in Ref. 8 our method does not rely on a priori knowledge of the dispersion and therefore not on linearization of the LLG equation. Thus, with our method we can explore the large  $\vartheta$  regime. The amplitude of the tilt of the magnetization in Eq. 4 is given by  $\vartheta$ . For large  $\vartheta$ , we expect to drive the system out of the linear regime. In Fig. 4 we show snapshots of the spin wave pattern at  $t = 1$  ns for six values of  $\vartheta$  and  $x_0 = y_0$ . See Supplemental Material at [URL will be inserted by publisher] for a video showing the spin wave dynamics after illumination of the sample with a circular spot  $x_0 = y_0 = 25 \mu\text{m}$  and  $\vartheta = 25^\circ$ .

We observe a strong dependence on the tilt angle  $\vartheta$ . For increasing values of  $\vartheta$ , features with a small spatial extent become visible near the center of the sample. These short-wavelength modes have a very large amplitude compared to the large-scale features. Furthermore, the symmetry of the spin wave pattern shows asymmetrical features. The asymmetry is due to the initial excitation given by Eq. 4 but for small values of  $\vartheta$  the asymmetry is not of appreciable size. For larger values of  $\vartheta$  the asymmetry becomes more pronounced.

The appearance of high-intensity small-scale features is also visible in the spin wave pattern with elliptical pulse shape, ( $x_0 \neq y_0$ ) as can be seen in Fig. 5 when compared with Fig. 3. The shape of the focal point is different in both cases and is determined by the initial conditions and the spin wave dispersion.

To interpret our numerical results we will briefly discuss the case when the dispersion becomes a function of the size of the spin wave amplitude  $\omega = \omega(k_x, k_y, |\varphi|^2)$  with  $|\varphi|^2 = m^2/(2M_S^2)$  the dimensionless envelope of the spin wave. Expanding the dispersion for small variations in the wavenumber and in the envelope term, we can derive the two dimensional nonlinear Schrödinger equation (NSE):<sup>24-27</sup>

$$i \left( \frac{\partial \varphi}{\partial t} + v_g \frac{\partial \varphi}{\partial x} \right) + \frac{1}{2} \beta_{2\parallel} \frac{\partial^2 \varphi}{\partial x^2} + \beta_{2\perp} \frac{\partial^2 \varphi}{\partial y^2} - N |\varphi|^2 \varphi = 0 \quad (6)$$

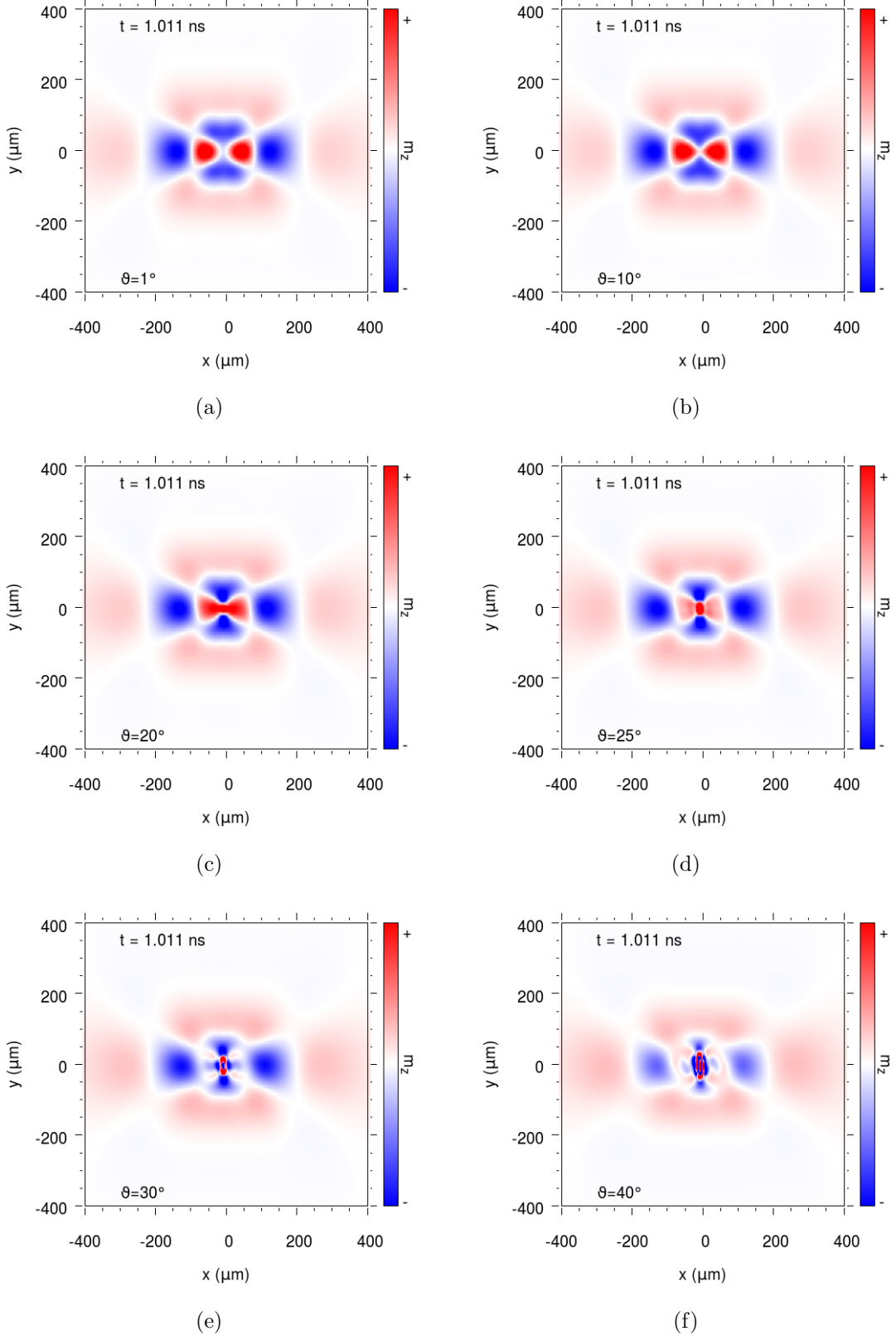


FIG. 4. Six snapshots of the spin wave pattern observed at  $t = 1$  ns with a circular initial excitation  $x_0 = y_0 = |\mathbf{r}_0| = 25\mu\text{m}$  and various values of  $\vartheta$ : (a)  $\vartheta = 1^\circ$ ; (b)  $\vartheta = 10^\circ$ ; (c)  $\vartheta = 20^\circ$ ; (d)  $\vartheta = 25^\circ$ ; (e)  $\vartheta = 30^\circ$ ; (f)  $\vartheta = 40^\circ$ . The color coding is scaled to the initial amplitude of the tilt  $\vartheta$  to aid comparison between the pictures. For increasing values of  $\vartheta$  the observed spin wave pattern features small wavelength modes near  $\mathbf{r} = 0$ .

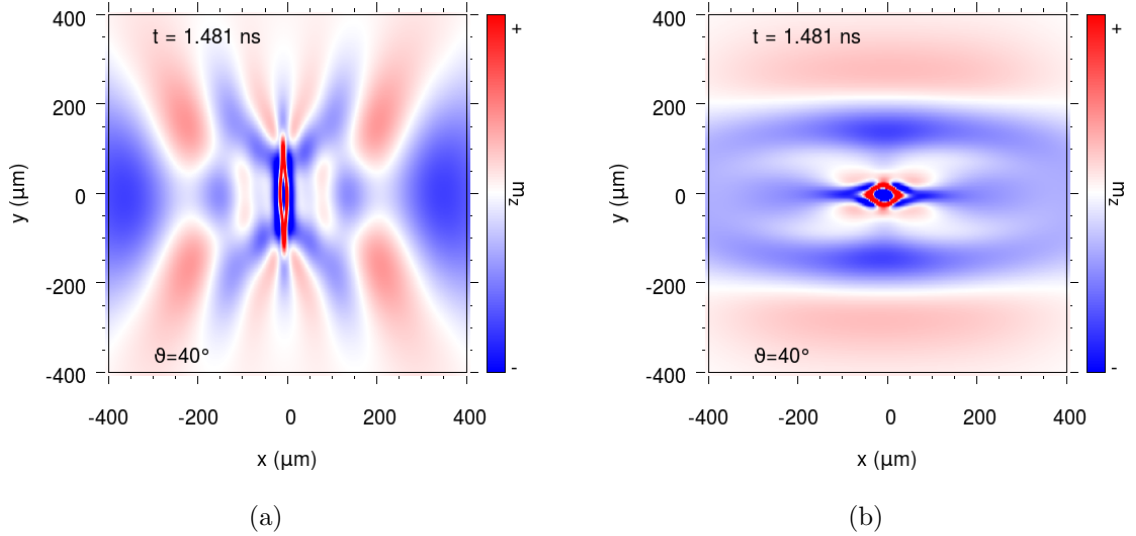


FIG. 5. Two snapshots at  $t = 1.5$  ns of the spin wave pattern for elliptical initial excitations as in Fig. 3 and  $\vartheta = 40^\circ$  with: (a)  $x_0 = 35\mu\text{m}$ ,  $y_0 = 140\mu\text{m}$ ; (b)  $x_0 = 140\mu\text{m}$ ,  $y_0 = 35\mu\text{m}$ . The color coding is scaled to the initial amplitude of the tilt  $\vartheta$  to aid comparison with Fig. 3. For these large values of  $\vartheta$ , the spin waves focus in the center of the beam spot. The spin wave dispersion determines the shape of the focus.

following the same notations as in Eq. 5, with

$$\begin{aligned}
 v_g &= \left. \frac{\partial \omega}{\partial k_x} \right|_{k=0} && \text{the group velocity,} \\
 \beta_{2\parallel} &= \left. \frac{\partial^2 \omega}{\partial k_x^2} \right|_{k_x=0} && \text{the dispersion coefficient,} \\
 \beta_{2\perp} &= \left. \frac{\partial \omega}{\partial (k_y)^2} \right|_{k_y=0} && \text{the diffraction coefficient}^{28}, \\
 \text{and } N &= \left. \frac{\partial \omega}{\partial |\varphi|^2} \right|_{k=0, |\varphi|=0} && \text{the nonlinear coefficient.}
 \end{aligned}$$

This equation does not include damping of the spin waves, which is always present in nature. It can be added to Eq. 6 if one includes a term proportional to  $i\alpha\varphi$  to the right hand side.<sup>13</sup> This makes the equation non-integrable and solutions can only be found using numerics. We will briefly discuss the possible solutions to Eq. 6 for the case  $\alpha = 0$  before returning to the damped case.

Solutions to Eq. 6 can exhibit behavior in which a continuous wave signal breaks down in an envelope of pulses<sup>29</sup>. This is called the modulation instability and can happen both in the direction of propagation (the longitudinal instability) as the direction perpendicular to wave propagation (the transverse instability).<sup>13</sup> Depending on the dispersion of the wave phenomena studied, these instabilities can give rise to stable solitonic solutions. These solutions are either self-channeling, i.e. the spin wave power is localized along a line, or self-focusing, where the wave power is localized in a single spot. This happens when nonlinear effects are counterbalanced either by dispersion or diffraction.<sup>11,24</sup> The balance is expressed in the *Lighthill* criterion:

$$\begin{aligned}\beta_{2\parallel}N < 0 & \text{ for longitudinal self modulation} \\ \beta_{2\perp}N < 0 & \text{ for transverse self modulation .}\end{aligned}$$

If a system allows both types of self-modulation the solutions are unstable and no solitons exist.<sup>11,13,15</sup> For both surface and volume magnetostatic waves the sign of  $N$  is always negative.<sup>24,27</sup> It is clear from the dispersion in Eq. 5 that both  $\beta_{2\parallel} < 0$  and  $\beta_{2\perp} < 0$ . Thus, the NSE has no stable solutions and self-modulation effects are not expected.

However, if damping is included in the analysis the situation is different. The previous unstable solution does not collapse upon itself since dissipation decreases the amplitude in time.<sup>15</sup> A quasi-stable spin wave packet can form for a limited amount of time, until the damping decreases the spin wave envelope below the threshold for nonlinearities. To observe the quasi-stable solutions for the BVMSW, the damping must be weak since it determines the lifetime of the quasi-stable solution but not be zero to avoid the collapse of the spin wave.

Returning to our numerical results of Fig. 4 and Fig. 5, we interpret our results as a manifestation of the quasi-stable self-focusing of nonlinear spin waves. The uniform approximation ensures that the Lighthill criterion is fulfilled in both transverse and longitudinal directions and the presence of a small damping stabilizes the nonlinearities. We have observed spin waves with a wavelength of a few  $\mu\text{m}$ , an order of magnitude smaller than the spatial dimensions of the optical pulse. The appearance of these small wavelength modes suggests that for large values of  $\vartheta$ , the system is pushed into the nonlinear regime. For circular excitations the Fourier transform of the excitation is a Gaussian with radius  $|\mathbf{k}_0| = 1/(2\pi|\mathbf{r}_0|)$ . When  $\vartheta$  is small, the distribution of modes in momentum space keeps this Gaussian profile.

However, for large values of  $\vartheta$ , modes with  $|\mathbf{k}| > |\mathbf{k}_0|$  become populated. To prove that these higher  $\mathbf{k}$  wavenumbers are the result of higher harmonics generation, we consider the time evolution of a plane wave excitation

$$\mathbf{m}(x, y) = m_0 \hat{\mathbf{e}}_x - \sin \vartheta \sin 2\pi \mathbf{r} \cdot \mathbf{k}_{\text{ini}} \hat{\mathbf{e}}_y, \quad (7)$$

with  $\mathbf{k}_{\text{ini}} = (0.01, 0.005) \mu\text{m}^{-1}$ . As before,  $m_0$  is a normalization constant ensuring  $|\mathbf{m}| = 1$  and  $\vartheta$  governs the amplitude of the sinusoidal modulation of the magnetization. In momentum space, this mode gives two sharp peaks at  $\pm \mathbf{k}_{\text{ini}}$ . We find that the distribution in momentum space does not change in time for  $\vartheta = 1^\circ$ . However, when we increase  $\vartheta$  to  $20^\circ$ , modes with integer multiples of  $|\mathbf{k}_{\text{ini}}|$  are present as shown in Fig. 6. Because the initial condition of Eq. 7 is periodic in space and our sample geometry is invariant under rotations around  $\hat{\mathbf{e}}_x$ , there is strong selection for wavenumbers that are odd multiples of  $\mathbf{k}_{\text{ini}}$ . The intensities fit an exponential envelope.

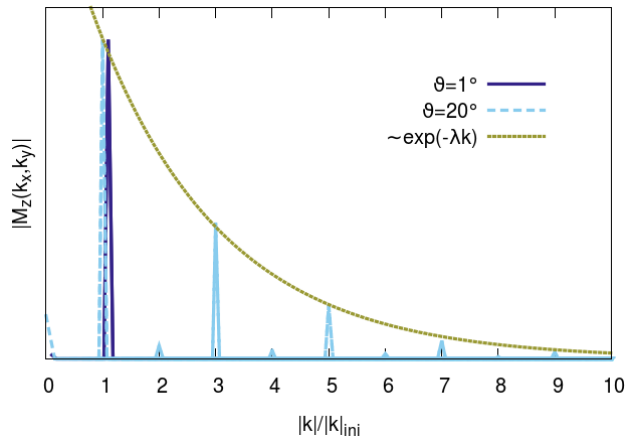


FIG. 6. Amplitude of  $M_z(\mathbf{k})$  along  $\mathbf{k}_{\text{ini}}$  averaged over approximately two full periods of precession for both  $\vartheta = 1^\circ$  (solid dark blue line) and  $\vartheta = 20^\circ$  (dashed light blue line). For easy comparison, we have normalized both spectra to the  $\mathbf{k}_{\text{ini}}$  peak and shifted the data for  $\vartheta = 1^\circ$ . For  $\vartheta = 1^\circ$ , the mode with initial wavevector  $\mathbf{k}_{\text{ini}}$  remains the only mode in the system, whereas at  $\vartheta = 20^\circ$  higher harmonics are clearly visible. Due to the symmetry of the initial condition, odd multiples of the initial wavevector are favored over the even multiples. The harmonics intensities fit an exponential envelope (dotted green line).

This confirms that for large values of  $\vartheta$ , higher harmonics are generated in the system, which shows that the system is in the nonlinear regime. The nonlinearities are also involved

in the enhancement of the asymmetry that occurs for large values of  $\vartheta$ . Since the dispersion is anisotropic, nonlinearity will have a dependency on the angle of propagation w.r.t. the external field. Nonlinear effects in the x-direction and the y-direction will be different and thus any initial asymmetry will become more pronounced.

#### IV. DISCUSSION

In this paper, we have presented numerical results on volume mode spin wave propagation in  $\text{Gd}_{4/3}\text{Yb}_{2/3}\text{BiFe}_5\text{O}_{12}$ . We modeled the effect of a femtosecond pulse of circularly polarized light by an instantaneous tilt in the saturation magnetization over an angle  $\vartheta$  in the direction perpendicular to the applied field and the equilibrium magnetization. Our simulations were performed in the uniform mode approximation and reproduce experimental results in the linear regime with very good agreement. For large values of  $\vartheta$ , we predict that nonlinear effects can lead to the appearance of small wavelength modes which are not present in the momentum distribution of the pump pulse. The small scale modes have a high intensity at the center of the pump spot. The spin wave dispersion in the uniform mode approximation allows for self-modulation effects since the Lighthill criterion is fulfilled and finite damping ensures the stability of the nonlinear solutions. The damping also plays an important role in the formation of the nonlinear solutions since the activation threshold of nonlinear behavior can be linked to the damping.<sup>30</sup>

Our results for small  $\vartheta$  coincide with experimental and computational results in the linear case<sup>8</sup> and predict self-focusing behavior and the generation of higher harmonics for larger  $\vartheta$ . Some comments on the experimental feasibility of these large  $\vartheta$  are in order.

A simple calculation shows that one requires a magnetic field of  $\sim 0.83$  T for 120 fs to tilt a single spin over an angle of  $1^\circ$ .<sup>31</sup> Since the pulse duration is three orders of magnitude shorter than the timescale of the volume mode spin wave dynamics, longer pulses increase the tilt angle without affecting the validity of our approach. Furthermore, since the IFE does not rely on absorption of the incident light, a larger tilt angle could be achieved by increasing the fluence of the pump pulse. For instance in the  $\text{DyFeO}_3$  garnet, a pulse of 200 fs with a fluence of  $500 \text{ mJ/cm}^2$  induced fields of 5 T.<sup>5</sup> Alternatively, the magnetization could be manipulated via the magnetic component of the pump pulse. Ref. 32 reported a tilt of  $0.4^\circ$  with a driving field of THz pulses peaking at 0.13 T. It has been suggested in Ref. 33

that by using higher-frequency optical pulses  $\sim 10$  T fields could be achieved, bringing the system in the nonlinear regime.

In the nonlinear regime, the self-focusing leads to large amplitude precession of the magnetization at the center of the pulse spot. The shape of the spin wave focus is determined by the spin wave dispersion  $\omega(\mathbf{k})$  and the shape of the incident beam. It is at least an order of magnitude smaller than the dimensions of the provided optical pulse. We hope that our predictions will stimulate pump probe experiments in the nonlinear regime and the study of self-focusing in the two dimensional plane with both high spatial and temporal resolution. Control of the spin wave flow in combination with nonlinear behavior could be useful in technological applications where a strong precession affects a local magnetic structure, such as in switching devices.

## ACKNOWLEDGMENTS

The authors want to acknowledge A. Kimel for his contributions at the start of the project. We want to thank T. Satoh and K. Shen for useful discussions. This work is part of the research program of the Foundation for Fundamental Research on Matter (FOM), which is part of the Netherlands Organization for Scientific Research (NWO). Furthermore, the work is supported by European Research Council (ERC) Advanced Grants No. 338957 FEMTO/NANO and No. 3398BEXCHANGE.

---

\* ltilburg@science.ru.nl

<sup>1</sup> M. Kammerer, M. Weigand, M. Curcic, M. Noske, M. Sproll, A. Vansteenkiste, B. Van Waeyenberge, H. Stoll, G. Woltersdorf, C. H. Back, *et al.*, Nat. Commun. **2**, 279 (2011).

<sup>2</sup> E. G. Tveten, A. Qaiumzadeh, and A. Brataas, Phys. Rev. Lett. **112**, 147204 (2014).

<sup>3</sup> R. Hertel, W. Wulfhekel, and J. Kirschner, Phys. Rev. Lett. **93**, 257202 (2004).

<sup>4</sup> P. S. Pershan, J. P. van der Ziel, and L. D. Malmstrom, Phys. Rev. **143**, 574 (1966).

<sup>5</sup> A. Kimel, A. Kirilyuk, P. Usachev, R. Pisarev, A. Balbashov, and T. Rasing, Nature **435**, 655 (2005).

<sup>6</sup> D. Popova, A. Bringer, and S. Blügel, Phys. Rev. B **84**, 214421 (2011).

- <sup>7</sup> A. Kirilyuk, A. V. Kimel, and T. Rasing, *Rev. Mod. Phys.* **82**, 2731 (2010).
- <sup>8</sup> T. Satoh, Y. Terui, R. Moriya, B. A. Ivanov, K. Ando, E. Saitoh, T. Shimura, and K. Kuroda, *Nature Photonics* **6**, 662 (2012).
- <sup>9</sup> F. Hansteen, A. Kimel, A. Kirilyuk, and T. Rasing, *Phys. Rev. B* **73**, 014421 (2006).
- <sup>10</sup> M. Bauer, O. Büttner, S. O. Demokritov, B. Hillebrands, V. Grimalsky, Y. Rapoport, and A. N. Slavin, *Phys. Rev. Lett.* **81**, 3769 (1998).
- <sup>11</sup> S. Demokritov, B. Hillebrands, and A. Slavin, *Phys. Rep.* **348**, 441 (2001).
- <sup>12</sup> M. Bauer, C. Mathieu, S. Demokritov, B. Hillebrands, P. Kolodin, S. Sure, H. Dötsch, V. Grimalsky, Y. Rapoport, and A. Slavin, *Phys. Rev. B* **56**, R8483 (1997).
- <sup>13</sup> J. Boyle, S. Nikitov, A. Boardman, J. Booth, and K. Booth, *Phys. Rev. B* **53**, 12173 (1996).
- <sup>14</sup> V. Demidov, J. Jersch, K. Rott, P. Krzysteczko, G. Reiss, and S. Demokritov, *Phys. Rev. Lett.* **102**, 177207 (2009).
- <sup>15</sup> O. Büttner, M. Bauer, S. Demokritov, B. Hillebrands, Y. S. Kivshar, V. Grimalsky, Y. Rapoport, and A. N. Slavin, *Phys. Rev. B* **61**, 11576 (2000).
- <sup>16</sup> L. D. Landau and E. M. Lifshitz, *Phys. Z. Sowjet.* **8**, 153 (1935).
- <sup>17</sup> E. R. Edwards, M. Buchmeier, V. E. Demidov, and S. O. Demokritov, *J. Appl. Phys.* **113**, 103901 (2013).
- <sup>18</sup> We are interested in the spin wave propagation in a 2 ns interval. The size of the lattice ensures that the spin waves do not reach the boundaries of the lattice during this interval.
- <sup>19</sup> F. J. Buijnsters, L. J. A. van Tilburg, A. Fasolino, and M. I. Katsnelson, *ArXiv e-prints* (2016), arXiv:1602.01362 [cond-mat.mes-hall].
- <sup>20</sup> J. H. Mentink, M. V. Tretyakov, A. Fasolino, M. I. Katsnelson, and T. Rasing, *J. Phys.: Condens. Matter* **22**, 176001 (2010).
- <sup>21</sup> M. d'Aquino, C. Serpico, G. Coppola, I. Mayergoyz, and G. Bertotti, *J. Appl. Phys.* **99**, 08B905 (2006).
- <sup>22</sup> M. Hurben and C. Patton, *J. Magn. Magn. Mater.* **163**, 39 (1996).
- <sup>23</sup> B. Kalinikos, *Microwaves, Optics and Antennas*, *IEE Proc. H* **127**, 4 (1980).
- <sup>24</sup> D. D. Stancil and A. Prabhakar, *Spin waves: Theory and Applications* (Springer, 2009).
- <sup>25</sup> G. B. Whitham, *Linear and nonlinear waves* (John Wiley & Sons, 1974).
- <sup>26</sup> V. I. Karpman, *Non-Linear Waves in Dispersive Media: International Series of Monographs in Natural Philosophy*, Vol. 71 (Elsevier, 2013).

- <sup>27</sup> A. Zvezdin and A. Popkov, Sov. Phys. JETP **2**, 350 (1983).
- <sup>28</sup> This term is usually written as the first derivative of  $\omega$  to  $k_{\perp}^2$ , absorbing the factor  $1/2$ , see Boyle *et al.*<sup>13</sup>.
- <sup>29</sup> V. Zakharov and L. Ostrovsky, Physica D **238**, 540 (2009).
- <sup>30</sup> A. N. Slavin, Phys. Rev. Lett. **77**, 4644 (1996).
- <sup>31</sup> J. Stöhr and H. C. Siegmann, Springer Ser. Solid-State Sci. , 5 (2006).
- <sup>32</sup> T. Kampfrath, A. Sell, G. Klatt, A. Pashkin, S. Mährlein, T. Dekorsy, M. Wolf, M. Fiebig, A. Leitenstorfer, and R. Huber, Nature Photonics **5**, 31 (2011).
- <sup>33</sup> A. Sell, A. Leitenstorfer, and R. Huber, Opt. Lett. **33**, 2767 (2008).